

Bandwidth Enhanced Operation of Photonic Time Delay Reservoir Computing

Irene Estébanez ⁽¹⁾, Janek Schwind ^(1,2), Ingo Fischer ⁽¹⁾, and Apostolos Argyris ⁽¹⁾

⁽¹⁾ Instituto de Física Interdisciplinar y Sistemas Complejos IFISC (CSIC-UIB), Campus UIB, 07122, Palma de Mallorca, Spain. (Corresponding author email: irene@ifisc.uib-csic.es).

⁽²⁾ Institute of Applied Physics, University of Münster, Corrensstr. 2/4, 48149, Münster, Germany.

Abstract We show numerically and experimentally that strong optical injection can enhance the operating bandwidth of semiconductor lasers with optical feedback in a photonic time-delay reservoir computing configuration. Its operating conditions can be significantly expanded while maintaining competitive computational performance in a time-series prediction task.

Introduction

Reservoir computing (RC) has proven to be a powerful method simplifying drastically the implementation and training of recurrent neural networks. Among the different hardware implementations^[1], time-delay reservoir computing (TDRC) represents a minimal design, with respect to hardware requirements and the training procedures^[2]. TDRC's ability for computation originates from time-multiplexing of recurrently connected virtual nodes that allows the storage of past information and, therefore, creating different responses depending on these previous inputs. While the process that feeds input into the reservoir and the connections within the reservoir are kept fix, supervised learning via linear regression is performed only at the reservoir's readout layer.

In the first part we numerically model a photonic TDRC. In particular, we use a semiconductor laser (SL) as the response laser which is biased just below threshold and is connected to an optical feedback loop (See Fig. 1). The information to be processed by this photonic structure is optically injected via a modulation applied to the optical carrier of an external drive laser^[3] Here we show that using strong optical injection, we can significantly expand the operating bandwidth of the reservoir, as well as the operating parameter

space for which we achieve efficient performance in an one-step-ahead nonlinear prediction task^[4]. In the second part we verify experimentally our findings.

Numerical modelling

The numerical modelling of the TDRC is based on the Lang-Kobayashi rate equations^[5], adapted to include an optical injection term that carries the information to be processed $J(t)$, multiplied by a mask $m(t)$ ^{[6],[7]}.

$$\frac{dE_r(t)}{dt} = \frac{1}{2}(1 + j\alpha)[G_r(t) - t_{ph}^{-1}] \cdot E_r(t) + \frac{r_c}{t_{in}} \cdot E_r(t - \tau)e^{j(\omega_0\tau + \varphi)} + \frac{r_{inj}}{t_{in}} \cdot E_{inj}(t)e^{j\Delta\omega t} \quad (1)$$

$$\frac{dN_r(t)}{dt} = \frac{I_r}{q} - \frac{N_r(t)}{t_s} - G_r \cdot |E_t|^2 \quad (2)$$

$$G_r(t) = g_n \cdot [1 + s|E_r(t)|^2]^{-1} \cdot [N_r(t) - N_0] \quad (3)$$

$$E_{inj}(t) = E_{inj,0} \cdot m(t) \cdot J(t) \quad (4)$$

The parameter notation and the corresponding values for the numerical calculations can be found in the analysis of [6]. The dynamical properties of this TDRC system can be controlled through certain key parameters. These are the feedback strength of the response laser r_c , the injection strength of the drive laser r_{inj} , and the optical frequency detuning between the drive and the response laser $\Delta f = f_d - f_r$. The time delay of the optical feedback loop in the photonic reservoir ($\tau = 16.8$ ns) is long enough to encode a sufficient number of virtual nodes for the TDRC tasks. By considering a time separation of $\theta = 100$ ps, a total number of $N = 168$ virtual nodes is available.

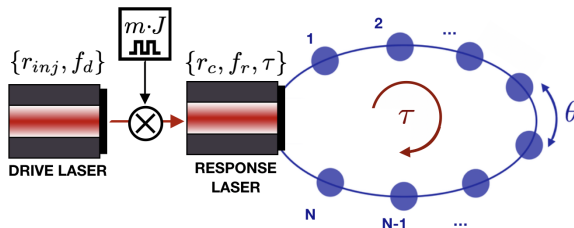


Fig. 1: A photonic reservoir built with a SL subject to time-delayed optical feedback, with N virtual nodes and equidistant time separation θ .

Computing task

We evaluate the impact of bandwidth enhancement of the photonic reservoir by testing the TDR capabilities in the one-step-ahead prediction task of the Santa Fe time-series^[4]. The way we input the information $J(t)$ into the virtual nodes of the delay line τ is via time-multiplexing. Each of the inputs is sampled and held for an interval θ and multiplied by a mask value, drawn from a random uniform distribution $[0,1]$, so masked input is expressed as $J(t) \cdot m(t)$. The mask is preserved for the whole task. The mask represents a fixed input connectivity and keeps the nonlinear responses of the reservoir laser in a transient regime.

The prediction output is obtained via training a linear classifier (ridge regression algorithm) at the output layer. From the Santa Fe data set, we use the first 3000 points as a training set, we skip the next 2000 points in order to obtain decorrelated training and testing data sets, while we use the following $L = 1000$ points as the testing set. The performance of the prediction task is evaluated by calculating the normalized mean square error (NMSE) between the target (input information) and the TDR prediction:

$$\text{NMSE} = \frac{1}{L} \sum_{n=1}^L (y(n) - \bar{y}(n))^2 \quad (5)$$

where the predicted value y , and the expected value \bar{y} are normalized to zero mean and unit variance.

Numerical results

As a first step, we evaluate the frequency response of the photonic reservoir. We define as metric for the operating bandwidth of the reservoir the frequency interval between low frequencies (excluding the DC contribution) and the high frequency which contains 80% of the total power spectral density of the emitted signal. To determine the operating bandwidth, we introduce random noise from a uniform distribution as input signal to the photonic reservoir for every iteration step of the numerical integration method (1 ps). The frequency response that is obtained within the $\{r_c, \Delta f\}$ parameter space, for two optical injection conditions (moderate, $r_{inj} = 0.4$ and strong, $r_{inj} = 2$), is depicted in Figure 2a and 2b, respectively.

We focus on an optical detuning regime $-30 \text{ GHz} < \Delta f < 5 \text{ GHz}$, where partial injection locking conditions are observed at the bound-

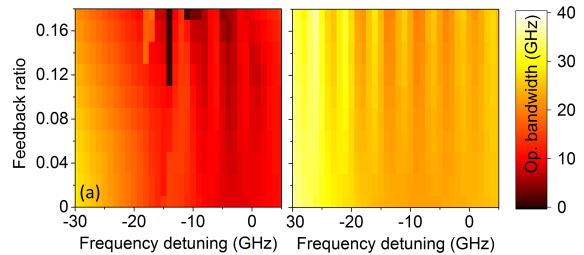


Fig. 2: Operating bandwidth (in GHz) of the photonic reservoir for (a) moderate ($r_{inj} = 0.4$) and (b) strong ($r_{inj} = 2$) optical injection conditions, in the $\{r_c, \Delta f\}$ parameter space.

aries. When comparing the two injection conditions, we observe that the operating bandwidth of the reservoir is systematically enhanced for the strong injection condition, compared to the moderate injection case. The operating bandwidth is an important property for reservoir computers that use the finite dynamical response time T of the reservoir laser to introduce coupling among the virtual nodes. This virtual node separation θ should be smaller than T , at the same time, θ should also not be chosen too small, to ensure sufficient response amplitudes. Previous works^{[2],[9],[10]} have demonstrated that a suitable choice for θ is approximately $0.2 \cdot T$. Moreover, favorable operating conditions of the photonic reservoir should also combine other important attributes for computing, such as fading memory and consistent nonlinear input/output signal transformation. For this reason, we evaluate the effect of the bandwidth enhanced operation on the task of Santa Fe one-step-ahead prediction for several conditions in the $\{r_c, \Delta f\}$ parameter space. In Fig. 3, we show the NMSE for the two cases of optical injection $r_{inj} = 0.4$ and $r_{inj} = 2$.

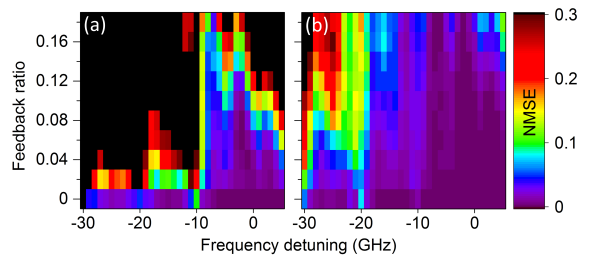


Fig. 3: NMSE performance for the Santa-Fe time-series prediction task in the parameter space $\{r_c, \Delta f\}$ for moderate ($r_{inj} = 0.4$) and strong ($r_{inj} = 2$) optical injection.

We find that strong injection conditions expand the the range of $\{r_c, \Delta f\}$ for which we achieve low NMSE performance. The injection locking regime is shifted to more negative frequency detuning (from -10 GHz to -20 GHz) while increasing injection strength, enlarging the region of partial locking that is usually associated with better reservoir performance^[11].

Experimental implementation

We also validate experimentally our claims, by implementing the photonic reservoir shown in Fig. 4. It has one input port that receives the masked information to be processed (input) and one output port from the photonic reservoir, that provides the signal for training and computation (output). The masked information $J(t) \cdot m(t)$ is uploaded into an arbitrary waveform generator (AWG) operating at 10 GSamples/s. That sets the separation between virtual nodes to $\theta = 100$ ps. The AWG's electrical output is amplified (RFA) and is modulated onto the optical carrier of the drive DFB SL, via a 20GHz Mach-Zehnder modulator (MZM). The operating frequency of the drive SL f_d is controlled by its operating temperature. The optical injection power that is fed to the response laser is controlled by a voltage controlled optical attenuator (ATT-1) that modifies the injection level r_{inj} . The polarization states of all optical carriers have been aligned. The response SL is biased at 11.8 mA (or at $0.995I_{th}$) and the frequency of its optical emission f_r is kept fixed. The optical feedback time delay of the photonic reservoir is $\tau = 16.8$ ns and includes an electrical variable optical attenuator (ATT-2) to tune the optical feedback strength r_c . The resulting signal is detected by a photoreceiver, and the electrical signal is recorded by a 16GHz (40 GSamples/s) real-time oscilloscope.

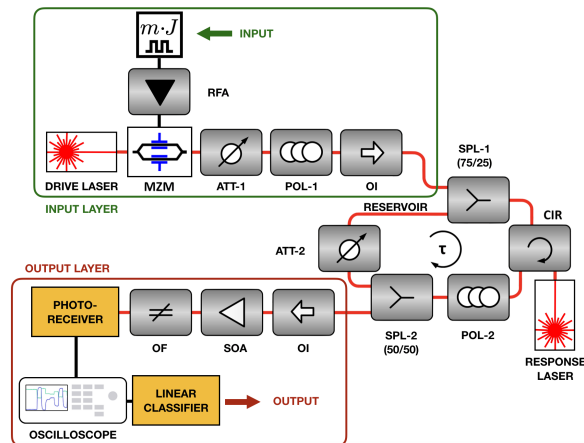


Fig. 4: Experimental configuration of the photonic TDR. POL: Optical polarization controller, SPL: Optical splitter, CIR: 3-port optical circulator, OI: Optical isolator, SOA: Semiconductor optical amplifier, OF: Tunable optical filter, OSC: Real time oscilloscope.

Experimental results

We repeat experimentally the same task we studied previously numerically. The linear readout classifier is implemented offline, by processing the reservoir's response signal acquired by the oscilloscope. The corresponding performance is

shown in Fig. 5. The characterization was performed versus frequency detuning Δf , for two different feedback ratios ($r_c = 0.02$ and $r_c = 0.04$) and for moderate ($P_{inj} = 0.125$ mW, Fig. 5A) and strong ($P_{inj} = 0.5$ mW, Fig. 5B) optical injection.

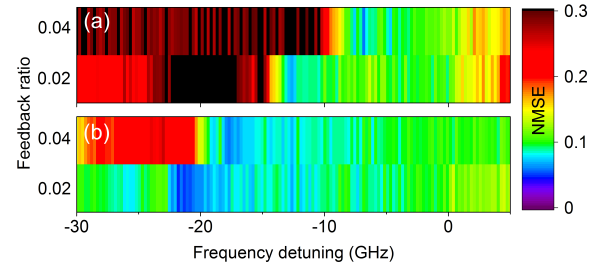


Fig. 5: NMSE performance for the Santa-Fe time-series prediction task in terms of frequency detuning Δf , for two different feedback ratios ($r_c = 0.019$ and $r_c = 0.035$) and for (A) moderate ($P_{inj} = 0.125$ mW) and (B) strong ($P_{inj} = 0.5$ mW) optical injection.

From the results of Fig. 5 we can demonstrate experimentally that strong optical injection yields a lower NMSE for expanded operating conditions of the reservoir parameters $\{r_c, \Delta f\}$. Again, we observe that the injection locking boundary, for which we find partial locking, shifts to more negative frequency detuning Δf , when injection becomes stronger.

Conclusions

We demonstrated numerically and experimentally the potential to enhance the operating bandwidth of a photonic TDR and to expand the operating region for which we obtain the best computing performance. While the performance of the investigated Santa Fe time-series computing task is preserved to the same levels, the tolerance of the reservoir's operating parameter space $\{r_c, \Delta f\}$ is significantly increased. This expansion is beneficial for real-world implementations of this system, as it provides higher robustness.

Acknowledgments

This work was supported by MINECO (Spain), through project TEC2016-80063-C3 (AEI/FEDER, UE) and by the Spanish State Research Agency, through the Severo Ochoa and María de Maeztu Program for Centers and Units of Excellence in R&D (MDM-2017-0711). The work of Dr. A. Argyris was supported by the Conselleria d'Innovació, Recerca i Turisme del Govern de les Illes Balears and the European Social Fund.

References

- [1] G. Van der Sande, D. Brunner, and M. C. Soriano, "Advances in photonic reservoir computing", *Nanophotonics*, vol. 6, no. 3, pp. 561–576, 2017.
- [2] L. Appeltant, M. C. Soriano, G. Van der Sande, J. Danckaert, S. Massar, J. Dambre, B. Schrauwen, C. R. Mirasso, and I. Fischer, "Information processing using a single dynamical node as complex system", *Nature Communications*, vol. 2, no. 468, 2011.
- [3] D. Brunner, M. C. Soriano, C. R. Mirasso, and I. Fischer, "Parallel photonic information processing at gigabyte per second data rates using transient states", *Nature communications*, vol. 4, no. 1, pp. 1–7, 2013.
- [4] A. S. Weigend and N. A. Gershenfeld, *Time series prediction: Forecasting the future and understanding the past: Proceedings of the nato advanced research workshop on comparative time series analysis*, 1992.
- [5] R. Lang and K. Kobayashi, "External optical feedback effects on semiconductor injection laser properties", *IEEE journal of Quantum Electronics*, vol. 16, no. 3, pp. 347–355, 1980.
- [6] K. Petermann, "External optical feedback phenomena in semiconductor lasers", *IEEE Journal of Selected Topics in Quantum Electronics*, vol. 1, no. 2, pp. 480–489, 1995.
- [7] J. Ohtsubo, "Semiconductor lasers: Stability, instability and chaos (series)", *Springer Series in Optical Sciences*, vol. 111, 2017.
- [8] I. Estébanez, J. Schwind, I. Fischer, and A. Argyris, "Accelerating photonic computing by bandwidth enhancement of a time-delayed reservoir.", *Nanophotonics*, vol. 1 (ahead-of-print), 2020.
- [9] M. C. Soriano, S. Ortín, L. Keuninckx, L. Appeltant, J. Danckaert, L. Pesquera, and G. Van der Sande, "Delay-based reservoir computing: Noise effects in a combined analog and digital implementation", *IEEE transactions on neural networks and learning systems*, vol. 26, no. 2, pp. 388–393, 2014.
- [10] S. Ortín and L. Pesquera, "Delay-based reservoir computing: Tackling performance degradation due to system response time", *Optics Letters*, vol. 45, no. 4, pp. 905–908, 2020.
- [11] J. Bueno, D. Brunner, M. C. Soriano, and I. Fischer, "Conditions for reservoir computing performance using semiconductor lasers with delayed optical feedback", *Optics Express*, vol. 25, no. 3, pp. 2401–2412, 2017.